High Power Density Actuation Through Terfenol-D Resonant Motion and Magnetorheological Flow Control

Brett Burton, David Nosse, Marcelo Dapino[1]
Department of Mechanical Engineering, The Ohio State University, Columbus, OH 43202

Abstract

There is currently a need for compact actuators capable of producing large deflections, large forces, and broad frequency bandwidth. In all existing transducer materials, large force and broadband responses are obtained at the price of small displacements and methods for transmitting very short transducer element motion to large deformations need to be developed. This paper addresses the development of a hybrid actuator which provides virtually unlimited deflections and large forces through magnetorheological (MR) flow control and rectification of the resonant mechanical vibrations produced by a magnetostrictive Terfenol-D pump. The device is a self-contained unit which produces large work output concurrently with stiffness and damping control, and is compact and self-locking when unpowered. To increase the output force, hydraulic advantage is created by implementing a driven piston diameter that is larger than the drive piston. Since the pump operates at high speeds in the low kHz range, a fast-acting MR fluid valve is required. The paper presents a four-port MR fluid valve in which the fluid controls its own flow while carrying the full transducer load. A prototype two-port valve was designed and constructed. Experimental measurements at various pressure levels are presented which demonstrate the new valve concept.

Keywords: Magnetorheological (MR) fluids, magnetostrictive pump, Terfenol-D, magnetorheological fluid valve, hydraulic advantage

1 Introduction

Increased performance requirements in traditional sectors such as automotive, aerospace, manufacturing and Department of Defense, in combination with new requirements in emerging fields such as nanotechnology and biotechnology, motivate the development of a new class of compact actuators which have high power density, few to no moving parts, and broad performance bandwidth. Some of the smart material transduction technologies being investigated can in certain cases exceed the power density of conventional electromagnetic devices, as is the case for example with the nickel titanium alloys. In these alloys, however, large displacements are obtained at the expense of small forces or slow frequency responses. Materials with faster reaction times, such as magnetostrictive or piezoelectric materials, have insufficient energy densities so applications based on these materials typically involve tradeoffs between displacement and force. Novel methods for converting very short motion into large deformations must therefore be developed.

The most advanced giant magnetostrictive materials produce static strains on the order of 1,600 microstrain at fields of 150 kA/m and loads of less than 14 MPa. Methods considered for amplifying these deformations include mechanical amplifiers [2] and inchworm concepts [9]. These methods, however, have some intrinsic problems such as wear and backlash and are thus unsuitable for applications which require maintenance-free operation or which are life-critical. The area of magnetorheological (MR) fluid dampers has grown considerably in recent years leading to innovative commercial products. However, MR fluids currently are not being employed commercially for actuation or sensing. Recent research efforts to that end include the work of Yoo et al. [14] on a piezohydraulic hybrid device, as well as other similar prototype devices [11]. Heating of the piezoceramic element has been shown to be one of the critical problems associated with piezohydraulic devices. Hybrid concepts which combine two classes of smart materials in a single device have been investigated before. Butler et al. [1] have shown that

[1]Correspondence: Email: dapino.1@osu.edu Ph.: (614)-688-3689 Fax: (614) 292-3163

Smart Structures and Materials 2004: Smart Structures and Integrated Systems,
edited by Alison B. Flatau, Proc. of SPIE Vol. 5390 (SPIE, Bellingham, WA, 2004)
0277-786X/04/$15 · doi: 10.1117/12.544566

the complementary electromechanical properties of piezoelectric and magnetostrictive materials can be used to enhance the bandwidth of a sonar transducer. Janocha and Clephas [6] have shown that the complementary electrical properties of these materials can lead to small increases in the overall transducer efficiency through reduction of the reactive power.

This paper presents a new class of compact actuators in which magnetostrictive materials and magnetorheological fluids are combined to produce large deformations and forces. The principle for achieving compact actuation is based on two effects: (i) rectification of resonant vibration produced by a magnetostrictive motor through magnetorheological flow control and (ii) utilization of hydraulic advantage for conversion of magnetostrain into large deflection and force. At this early stage in the actuator development program, it is estimated that this technology will provide a performance space comparable to that of pneumatic actuators, but it is noted that an important advantage of the actuator presented here over pneumatic systems is that it does not require external support systems such as compressors and supply lines. Furthermore, the actuator might produce larger net forces than pneumatic actuators to a degree comparable to those produced by low range hydraulic systems while being free of wear and backlash problems. In combination with the self-contained design, these features will lead to actuators with enhanced functionality, higher energy density, broader frequency bandwidth, minimal redundancy requirements, and higher reliability.

Applications which can benefit from this new actuator technology include, among others, compact haptic interfaces, control surfaces for unmanned vehicles, heavy duty actuator-based suspension components for terrestrial vehicles, adaptive airframes, and robotic locomotion components. Advantages of the hybrid actuator presented here include: (i) large work output concurrently with stiffness and damping control; (ii) ability to not only actuate but also sense via force feedback properties; (iii) virtually continuous motion; (iv) fail-safe design since the device is self-locking when unpowered; (v) fly-by-wire design enables reduced redundancy; (vi) high energy density and compact packaging; and (vii) output displacement which is limited by the geometry as opposed to by the active materials.

The specific focus of the paper lies in the development of a suitable magnetorheological fluid valve with a view to be able to magnetically control the flow of MR fluid in an on/off fashion. Given the fact that the actuator operates on the principle of mechanical rectification of vibrations in the low-kHz range, the valve must provide fast responses. This in fact precludes the use of mechanical valves and justifies the use of magnetically activated materials. In Sec. 2 is presented the principle of operation of the hybrid actuator. The design and modeling aspects of the MR fluid valve are discussed in Sec. 3, while the corresponding considerations for the Terfenol-D pump are highlighted in Sec. 4. The experimental results are presented in Sec. 5, while the conclusions of this study and future work are discussed in Sec. 6.

2 Principle of Operation of the Hybrid Actuator

Magnetorheological (MR) fluids are suspensions of micron-sized magnetic particles - typically spherical iron particles - in a carrier fluid. The magnetorheological response of an MR fluid originates in the magnetization of the suspended particles in response to magnetic fields [8, 12]. The close range interaction among neighboring particles causes the particles to form chain-like columnar structures in directions parallel to the magnetic flux, as shown in Fig. 1. These structures lead to an increase in the apparent viscosity of the suspension by restricting the flow along directions perpendicular to the applied field. The mechanical energy needed to break the columnar chains increases as the field is increased and in agreement with the magnetic nature of the particles, the dependence of yield stress with field exhibits saturation and a slight amount of hysteresis. In the absence of magnetic fields, MR fluids exhibit Newtonian behavior.

Due to the magnetic field actuation, the reaction times of MR fluids are very short and are primarily controlled by the overall inductance of the fluid and surrounding magnetic circuit. Eddy current losses are relatively small in MR fluids as well, which is advantageous for achieving broad frequency bandwidths. This also implies that

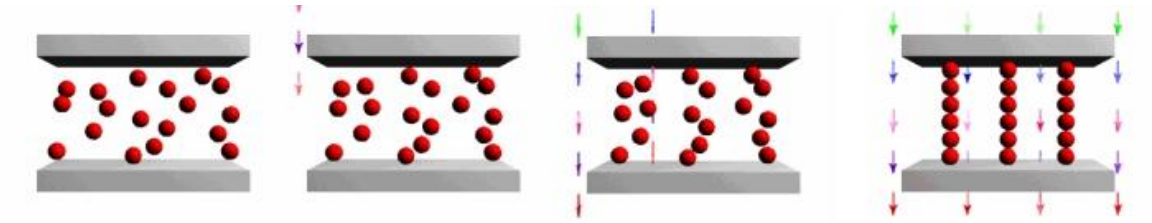

No Field Maximum Field

Figure 1: Sequence showing the alignment of iron particles with respect to an external magnetic field (Lord Co.)

the Terfenol-D element must be laminated. To maximize the response of the Terfenol-D pump, the drive field must have a frequency equal to one-half the resonance frequency of the Terfenol-D element since the pump is driven unbiased at full stroke.

Figs. 2(a)-(c) show the hybrid magnetostrictive-magnetorheological actuator, which consists of a four-port magnetorheological fluid valve, magnetorheological fluid, Terfenol-D pump, drive piston, and driven piston. To achieve rectification of the resonant vibrations produced by the Terfenol-D pump, and thus large deflections, the actuator operates through cyclic repetition of two stages, actuator extension and fluid refill. At each stage the MR fluid valve completely closes one half of the fluid circuit and permits free flow through the other half.

The MR fluid valve has two conical ends, each fitted with permanent magnets for driving the MR fluid. Solenoids wrapped around the valve at each end are used to cancel the field produced by the permanent magnets, therefore creating a normally-on mechanism that locks the actuator in the event of power failure. When the solenoid around the valve has no applied current, there is no magnetic field cancelation and the MR fluid increases in viscosity. When a suitable current is applied, the coil's magnetic field cancels the permanent magnet's field and the MR fluid decreases in viscosity, thus permitting flow through the valve. The actuator extension stage commences with the leftmost solenoid turned on and the rightmost turned off, as shown in Fig. 2(b). This effectively thickens the MR fluid in the right path, producing a fluid path of least resistance through the left valve half. The flow produced by the Terfenol-D pump produces a pressure differential that fully closes the right valve. Once closed, the flow extends the driven piston for positive actuation. To increase the output force, a hydraulic advantage is created by implementing a driven piston diameter that is larger than the drive piston.

The fluid refill stage immediately follows as the Terfenol-D element and drive piston begin to retract, see Fig. 2(c). To refill the fluid cavity without also retracting the actuator output, the left solenoid is turned off and the right turned on. This changes the fluid path of least resistance and creates the pressure differential necessary to begin closing of the leftmost valve half. With the left half closed, the actuator output is temporarily locked, and the free flow path through the opened right valve refills the cavity. Steps (b) and (c) are subsequently repeated at high speed to further extend the driven piston and thus achieve almost continuous motion of the load attached to the actuator. Figure 3 shows the timing diagram for the Terfenol-D pump and MR fluid valve.

3 Magnetorheological Fluid Valve Design

The successful implementation of the hybrid actuator hinges on the ability to control the flow of magnetorheological fluid between full and null flow by means of a four-port valve. The pressure differential across the valve depends on the ratio of the piston areas, magnetorheological fluid properties, magnetic field intensity, and magnetorheological fluid pressure. To accommodate these behaviors, MR fluids are often modeled as a Bingham plastic having a variable yield strength, [8]

$$\tau = \tau_y(H) + \eta\dot{\gamma} \quad \tau > \tau_y, \tag{1}$$

$$\tau = G\gamma \quad \tau < \tau_y, \tag{2}$$

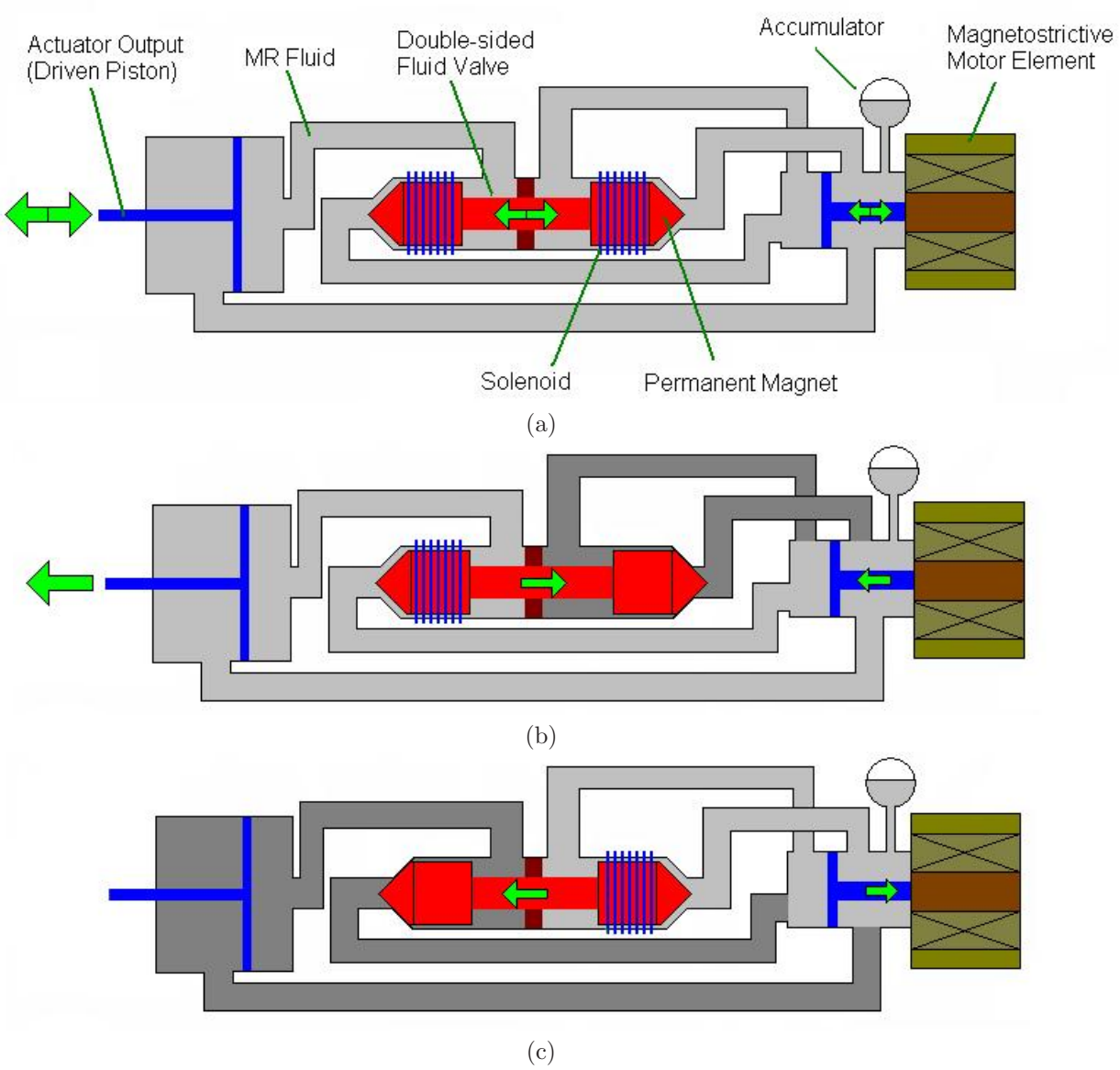

Figure 2: (a) Hybrid magnetorheological fluid-magnetostrictive actuator. In (b), the drive piston connected to the Terfenol-D pump pushes the fluid through the left valve half and subsequently pushes the driven piston on the load end (left coil active), while the right valve half remains closed. In (c), the drive piston retracts while the MR fluid recirculates through the right half valve (right coil active). The driven piston stays fixed until step (b) starts again and the sequence is repeated. Permanent magnets inside the conical heads provide a bias force on the MR fluid.

where τ_y is the field dependent yield stress, γ and τ represent the shear strain and stress, G is the complex material modulus, $\dot{\gamma}$ is the shear rate, and η is the zero field viscosity. Although real MR fluids exhibit some departures from the behavior predicted by the Bingham plastic model, especially concerning non-Newtonian behaviors often observed in these fluids, [10] the Bingham model provides a starting point for studying the suitability of commercial MR fluids for use in the hybrid actuator presented here.

Referring to the actuator architecture shown in Fig. 2, the total actuator length is primarily determined by the size of the driven piston, which is in turn determined by the prescribed displacement. Assuming a commercial

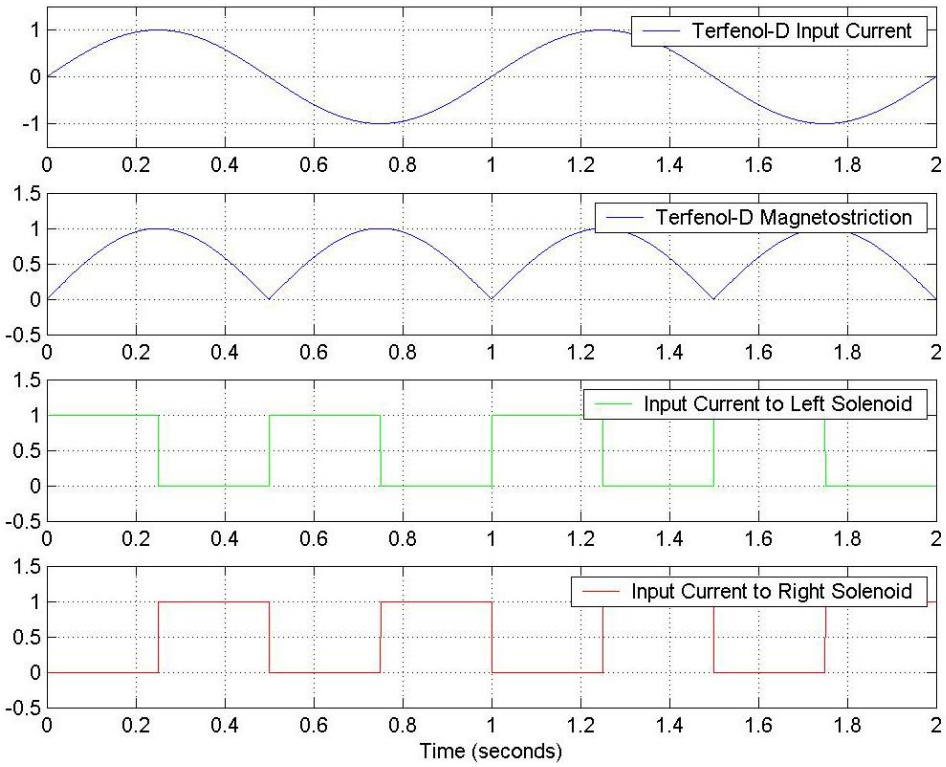

Figure 3: Timing diagram for the Terfenol-D pump and MR fluid valve.

MR fluid with properties as shown in Fig. 4, a standard 1 in (25.4 mm)-long Terfenol-D rod, a prescribed load $F_L = 3$ kip (13.4 kN) and a maximum load travel of 4 in, the total device length is approximately 7 in. Employing a Bingham plastic model, the pressure differential in an MR flow on a surface $W \times L$ is given by

$$\Delta P = \Delta P_\eta + \Delta P_\tau = \frac{12\eta Q L}{g^3 W} + \frac{c\tau_Y L}{g}$$

where Q is the volumetric flow and g is the gap between the two magnetic poles. The term ΔP_η represents the zero-field pressure drop and ΔP_τ represents the field-dependent pressure drop across the valve.

Assuming the dimensions $W = 0.25$ in, $L = 0.5$ in, $g = 1/16$ in, $\eta = 0.25$ Pa.s, $Q = 8.806 \times 10^{-3}$ gal/s, and the material properties $c = 3$ and $\tau_Y = 40$ kPa, one obtains

$$\Delta P_\eta = 50 \text{ kPa},$$

$$\Delta P_\tau = 800 \text{ kPa}$$

and

$$\Delta P = 1.130 \text{ MPa}.$$

In order to determine the design parameters necessary for achieving this pressure drop, two cases are considered. In the first, the magnetostrictive pump is assumed inactive (failure condition) while in the second, the pump is assumed to provide its blocking force (blocked strain condition.)

Case A. The pressure drop is equal to $\Delta P = F_L/A_L = 1.130$ MPa thus the cross section is $A_L = 0.0118$ m^2 and the diameter becomes $D_L = 0.122$ m. This is the driven piston diameter needed to avoid failure of the pump.

Case B. The magnetostrictive blocking force is $F_{blk} = (E_Y^B A/L)\lambda_s$ where E_Y^B is the elastic modulus at electrical open circuit and A and L respectively denote the area and length of the magnetostrictive rod. Assuming

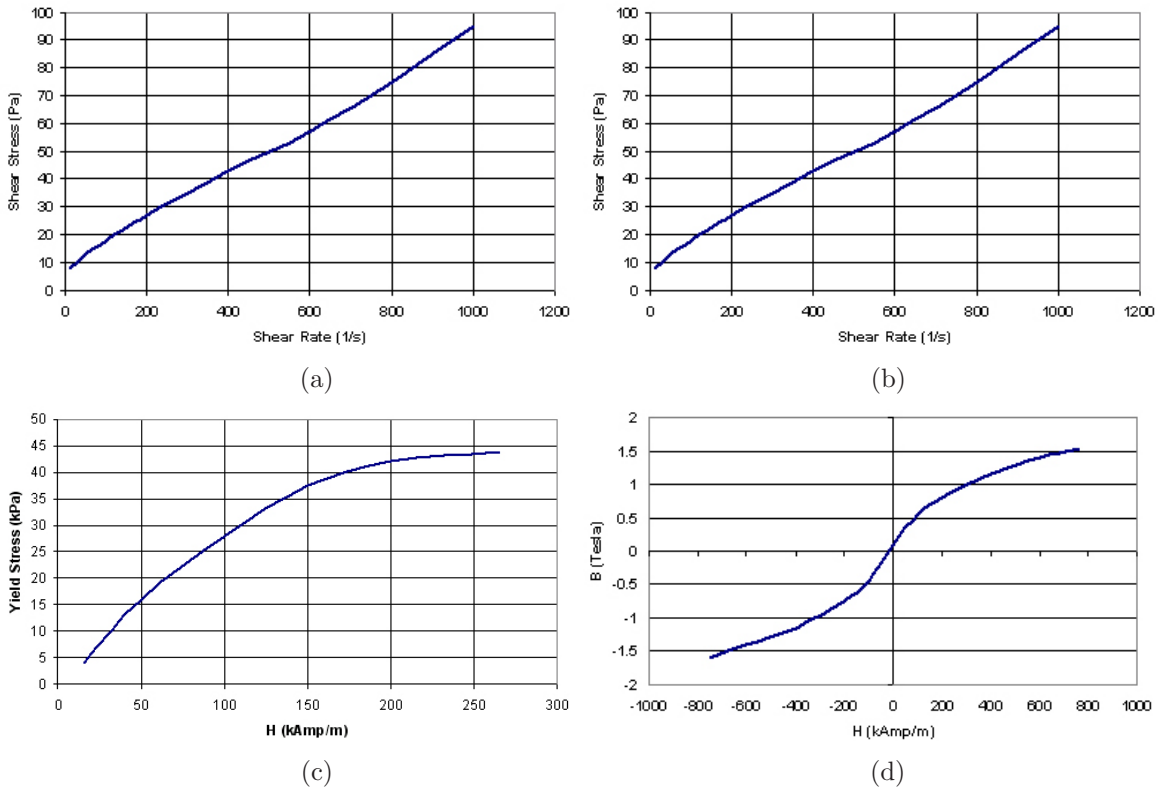

Figure 4: Mechanical and magnetic properties of Lord's hydrocarbon-based MR fluid MRF-132AD.

nominal Terfenol-D parameters, one obtains $F_{blk} = 500$ N. Assuming a driven piston area $A_M = A$, the pressure on the magnetostrictive motor becomes $P_M = 3.78$ MPa. On the load side, since $P_L = 13,345/A_L$, one obtains $\Delta P = 13,345/A_L - 3.78 \times 10^6 = 1.13 \times 10^6$ Pa, thus $A_L = 2.718 \times 10^{-3}$ m^2 and $D_L = 0.06$ m $= 2.4$ in. Therefore, the necessary clamping force is achieved with a piston diameter on the load side of 2.4 in or 6 cm.

The magnetic circuit in the magnetorheological fluid valve was designed using finite element analysis (femm 3.2.) The flux lines around the conical end of the valve are shown in Fig. 5, where it is noted that in this simulation two series coils are employed to drive the MR fluid instead of permanent magnets. While in the design used here the coils must be excited continuously to achieve self-locking operation, the coils provide more control for adjusting the intensity of the field than permanent magnets do. This design was therefore implemented first for development purposes. The model was constructed assuming axisymmetric responses and the MR fluid's magnetization versus field curve shown in Fig. 4(d) was incorporated by means of a nonlinear look up table.

4 Terfenol-D Motor Design

The model approach considered here involves the characterization of the mechanisms that govern magnetomechanical hysteresis in a Terfenol-D pump driven at mechanical resonance. A general description of the model is provided in Table 1; further details can be found in [4, 5]. In this model, magnetic hysteresis is assumed due to a restraining effect of pinning sites on domain walls as the latter attempt to translate in response to applied magnetic fields. Following the original work of Jiles and Atherton [7], relations (3)-(7) are constructed from a thermodynamic balance between the magnetic energy supplied to a ferromagnet, the actual or prevailing magnetostatic energy, and the energy lost to pinning. In ideal defect-free materials, that is materials devoid of cracks,

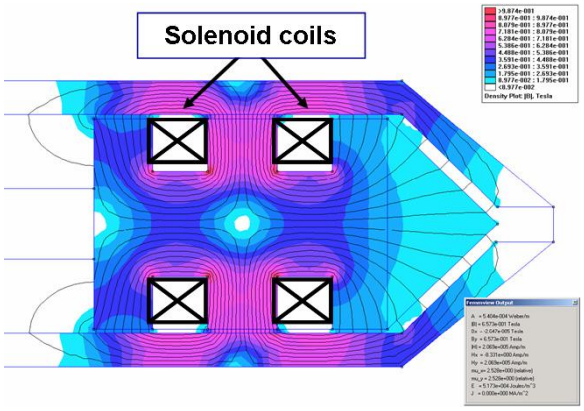

Figure 5: Finite element calculations showing the magnetic flux lines on the conical head of the magnetorheological fluid valve.

Table 1: Coupled structural-magnetic model for the design and control of the Terfenol-D pump.

Magnetic Kernel:

$$\alpha(M,\sigma) = 3/(2\,\mu_0\,M)\,\partial(\sigma\,\varepsilon)/\partial M \tag{3}$$

$$M_{an}(t,x) = M_s\,\left[\coth\left(\frac{H(t,x)+\alpha(M,\sigma)\,M(t,x)}{a}\right) - \left(\frac{a}{H(t,x)+\alpha(M,\sigma)\,M(t,x)}\right)\right] \tag{4}$$

$$\frac{\partial M_{irr}}{\partial t}(t,x) = \left\{\zeta\,\frac{M_{an}(t,x)-M_{irr}(t,x)}{\delta\,k-\alpha(M_{irr},\sigma)\,[M_{an}(t,x)-M_{irr}(t,x)]}\right\}\frac{dH}{dt}(t,x) + \left\{\frac{\sigma(t,x)}{E\,\xi}\,[M_{an}(t,x)-M_{irr}(t,x)]\right\}\frac{d\sigma}{dt}(t,x) \tag{5}$$

$$M_{rev}(t,x) = c\,[M_{an}(t,x)+M_{an}(t,x)] - c\,M_{irr}(t,x) \tag{6}$$

$$M(t,x) = (1-c)\,M_{irr}(t,x) + c\,[M_{an}(t,x)+M_{an}(t,x)] \tag{7}$$

Structural Kernel:

$$\lambda[M(t,x)] = (3/2)\,\lambda_s\,(M/M_s)^2(t,x) \tag{8}$$

$$\int_0^L \rho\,A\,\frac{\partial^2 u}{\partial t^2}(t,x)\phi(x)\,dx = -\int_0^L \left\{c_D\,A\,\frac{\partial^2 u}{\partial x\partial t}(t,x) + E\,A\,\left[\frac{\partial u}{\partial x}(t,x)-\lambda(t,x)\right]\right\}\frac{\partial\phi}{\partial x}(x)\,dx - \left[m_L\,\frac{\partial^2 u}{\partial t^2}(t,L) + c_L\,\frac{\partial u}{\partial t}(t,L) + k_L\,u(t,L) + F_{ext}(t)\right]\,\phi(L) \tag{9}$$

$$\varepsilon(t,x) = \partial u/\partial x(t,x) \tag{10}$$

$$\sigma(t,x) = E\,\frac{\partial u}{\partial x}(t,x) + c_D\,\frac{\partial^2 u}{\partial x\partial t}(t,x) - E\,\lambda(t,x) + \sigma_0 \tag{11}$$

$$Q\,\ddot{\vec{U}}(t) + C\,\dot{\vec{U}}(t) + K\vec{U}(t) = \vec{F}(t) \tag{12}$$

crystal twinning, stress discontinuities, etc., no magnetizing energy is lost. Upon cycling of magnetic field H, magnetization M describes anhysteretic paths M_{an} characterized by local or global energy minima. Such paths are described in this model by the Langevin equation [7]. That the magnetization M of a ferromagnet exhibits both reversible M_{rev} (energetically conservative) and irreversible M_{irr} (dissipative) components has been long

recognized. In the Jiles-Atherton model, reversible components take place when magnetic field levels are low and pinning energy dominates domain wall energy. Under these conditions, domain walls bulge reversibly as the field is cycled, while remaining attached to pinning sites. Upon application of moderate to large fields, domain walls may attain sufficient energy to overcome the restraining force of pinning sites resulting in domain walls unattaching from low energy sites and attaching to remote sites. As this motion occurs, domain walls must climb higher energy potentials and energy is effectively lost. Hence, additional external energy must be provided to compensate for the unpinning and pinning of domain walls. This energy loss manifests itself in the form of hysteresis and its magnitude can be determined from the area under the M vs. H characteristic curve. Stress has a "wiping out" effect on hysteresis since it contributes to domain wall unpinning [13]. Equations (3)-(7) describe these phenomena under isothermal conditions. Here, k is the average pinning energy, c is a reversibility coefficient, ξ is the approach coefficient, and ζ ensures that hysteresis energy is always dissipative.

The second magnetomechanical component to be modeled is the deformations that occur when domain configurations change in response to an applied field H. These deformations can be modeled through either energy or empirical formulations [3]. While most energy methods yield accurate solutions, the stochastic nature of the domain configurations makes this approach computationally expensive and generally unfeasible for device design and control. For this reason, the isotropic single-valued relation (8) is employed. Here, λ_s and M_s respectively denote the saturation magnetostriction and saturation magnetization. It is noted that this expression yields very accurate results when the mechanical preload is sufficiently high to prealign magnetic moments in directions perpendicular to easy crystallographic axes.

Relation (8) quantifies the reorientation of magnetic moments toward the magnetization direction. It was shown [5] that λ in (8) is analogous to the term $d_{33}H$ in the linear piezomagnetic model $\varepsilon = s^H \sigma + d_{33} H$. One major difference is that λ is inherently nonlinear and hysteretic through both the magnetization M and the fact that λ vs. M is quadratic. For this coupled magnetomechanical model to be complete, however, the elastic properties of the vibrating Terfenol-D element be considered. Such properties are represented in the linear piezomagnetic model by $s^H \sigma$. Referring to Figure 6, in which displacements $u(t,x)$ are defined relative to the preloaded deflection produced by preload stress σ_0, force balancing relation (11) is used to derive a dynamic PDE model quantifying the rod dynamics. This PDE has the form of a wave equation with magnetostrictive inputs and boundary conditions $u(t,0) = \dot{u}(t,0) = 0$ and force equilibrium, $\sigma(t,L) = 1/A\,[-k_L\,u(t,L) - c_L\,\partial u/\partial t(t,L) - m_L\,\partial^2 u/\partial t^2(t,L)]$, for all t. To numerically approximate the displacement solutions, the PDE model is first expressed in weak or variational form in relation (9). In this equation, ρ is the mass density, A is the rod cross-sectional area, c_D is the Kelvin-Voigt damping coefficient, and $F_{ext}(t)$ is an external force which characterizes the transducer as a force sensor. A subsequent Galerkin finite element discretization yields the second-order time-dependent vector system given by relation (12). Here, Q, C and K respectively denote the mass, damping and stiffness matrices. A simple trapezoidal method is then used for obtaining rod displacements $u(t,x)$ and strains $\varepsilon(t,x)$ - relation (10).

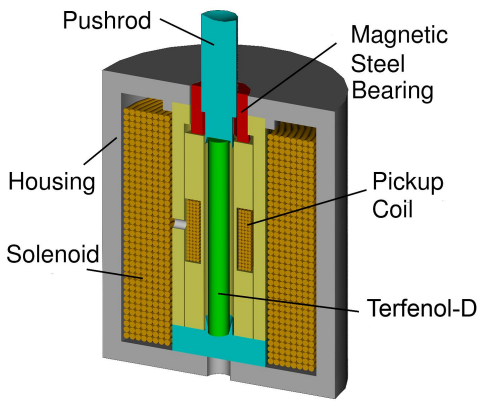

Figure 6: Rendering of the Terfenol-D motor employed in the hybrid actuator.

5 Experiments

The primary focus at this early stage in the investigation is to demonstrate the feasibility of the MR fluid valve, especially concerning the ability of the valve to control the flow under both low and high pressures. Since the valve operation is governed by both the pressure differential across the valve and the change in viscosity of the MR fluid, the low pressure tests gage the ability of the MR fluid to provide sufficient blocking of the flow to allow the valve to close. Conversely, under high pressure differentials the valve must completely impede the flow while the magnetic field is applied and allow the MR fluid to flow freely through the valve once the field is removed. It is emphasized that for development purposes, a normally-off design based on solenoid coils was employed since coils provide more control for adjusting the intensity of the field than permanent magnets do.

For proof of the concept purposes, a prototype MR fluid valve was constructed as shown in Figs. 7 and 8. The prototype is a one-half version of the full valve and is fitted with a helical spring which provides a return mechanism. Pressure to the system is applied with a nitrogen tank and a cylindrical piston which acts as a pressure amplifier and as an interface between the nitrogen and MR fluid. The pressurized MR fluid is fed into the MR fluid valve by means of a pressure control valve, while a pressure sensor (Sensotec GM-A 922453) records the pressure during the experiments. The voltage to the coils is supplied by a dc power source (Tektronix CPS250) and linear amplifier (MB Dynamics SL500VCF). The motion of the valve is measured with a contactless displacement sensor (SA1D-LK4), aimed at the back of the valve's shaft. Measured signals include fluid pressure, shaft displacement and voltage at the coils.

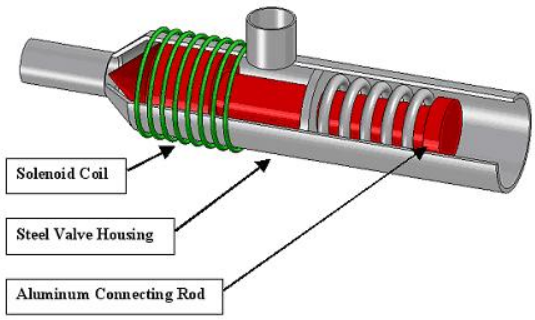

Figure 7: Illustration showing the single-sided MR fluid valve constructed for proof of the concept analysis.

In Fig. 9(a) the ability of the valve to close and hold pressure at 800 psi is shown. A dc voltage of 20 V was first applied and quickly removed after two seconds. The pressure control valve was subsequently opened and it is observed that the MR fluid valve shut completely without leakage. In this case, the hydraulic pressure alone is sufficient to drive the valve. This principle will be used in the double-sided valve (see Fig. 2) to drive the valve back and forth by directing the hydraulic pressure to either side of the valve. At high pressure levels, whether or not the field is applied is inconsequential as shown in Fig. 9(b), where a pressure of 600 psi was used. It is clear from Figs 9(a)-(b) that the valve design allows for closure of the flow at high pressures. However, it is necessary to show that the closure is ensured at low pressures. The change in viscosity of the MR fluid under the action of magnetic fields is used to that end. This is shown in Fig. 10(a), where a line pressure of 25 psi was used. The valve closes as the field is applied and remains in that state after the field is removed. In Fig. 10(b), the field was applied first and a pressure of 150 psi was applied thereafter.

The operation of the valve must be bidirectional as the magnetic field is cycled in combination with controlled fluctuations in the hydraulic pressure. Fig. 11 shows the response of the valve as the field is sequentially stepped up and down three times. The measured valve displacement closely follows the field. For the second and third steps, there is a decay in both the line pressure and valve displacement which is due to the finite amount of MR fluid in the pressure amplifier chamber. Such steps will not occur in the finished actuator as the MR fluid will be continuously recirculated.

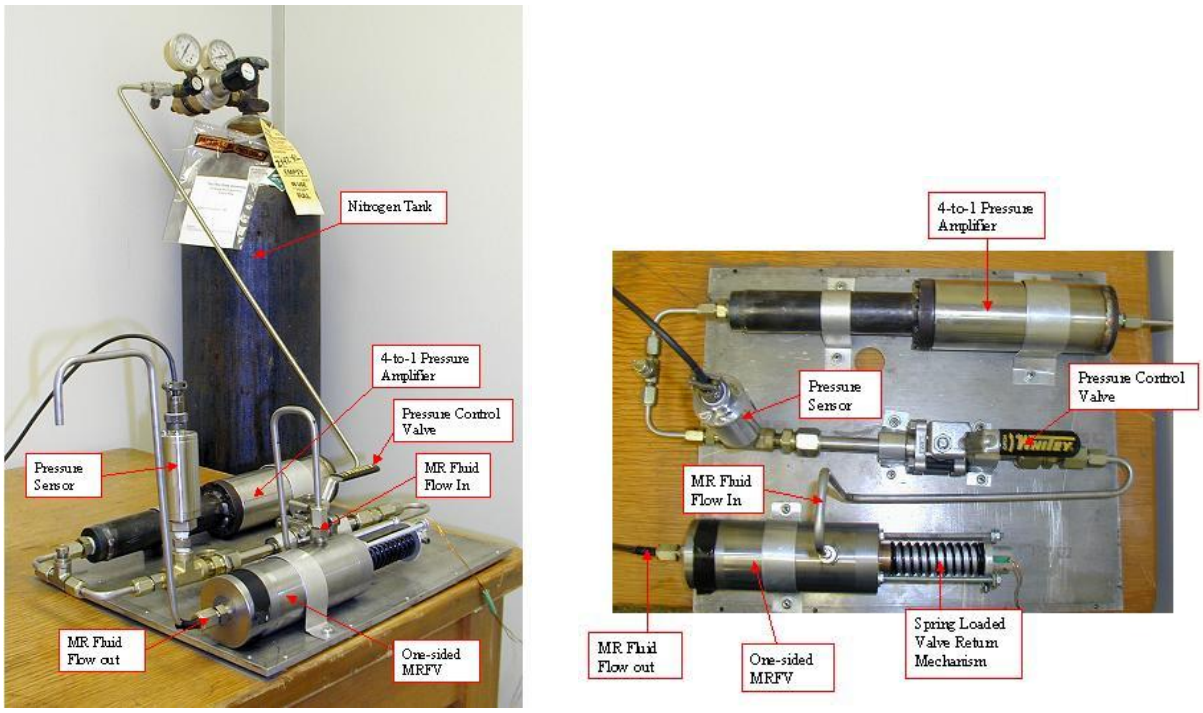

(a) (b)

Figure 8: (a) Experimental setup used for testing the MR fluid valve. (b) Detailed view.

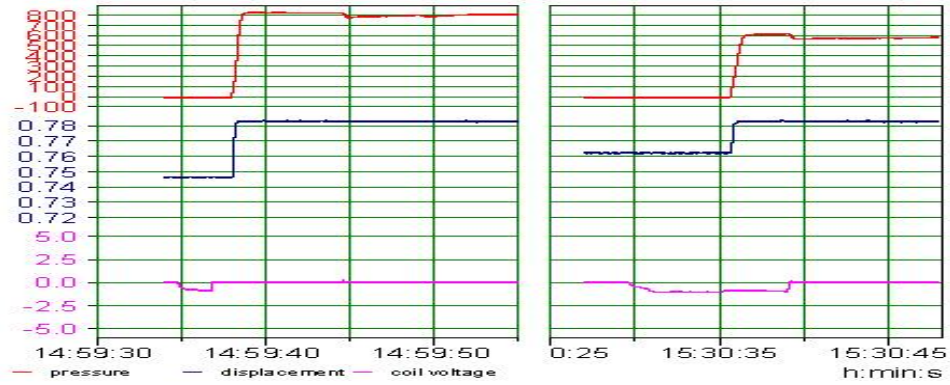

(a) (b)

Figure 9: Pressure, displacement and coil voltage signals. (a) 800 psi test and (b) 600 psi test.

6 Conclusions and Future Work

The experimental measurements conducted on the prototype two-port (single sided) magnetorheological fluid valve demonstrate the feasibility of the novel hybrid transducer concept presented here. These results represent the first step toward the development of the actuator. In the next step, we will develop a two-port (double sided) valve, which will be tested under both static and dynamic loads with the goal of being able to develop the speeds required for achieving a smooth rectification of the Terfenol-D vibrations. This step will be accompanied by a more comprehensive model development effort aimed at better establishing design criteria for miniaturizing the various transducer components, especially the MR fluid valve itself.

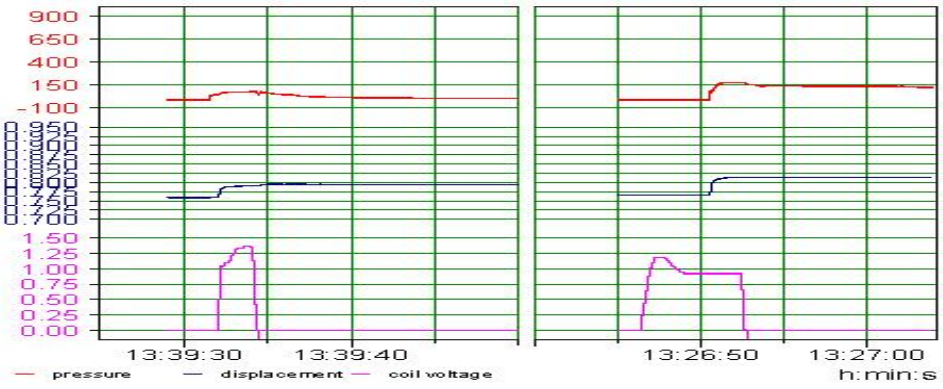

(a) (b)

Figure 10: Pressure, displacement and coil voltage signals. (a) 25 psi test and (b) 150 psi test.

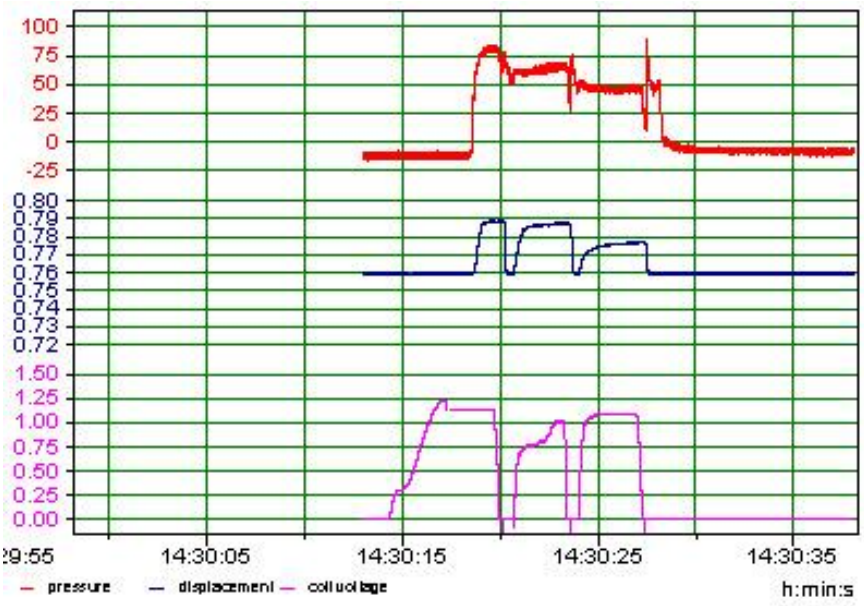

Figure 11: Pressure, displacement and coil voltage signals, cyclic test at 90 psi test.

Acknowledgements

This work was supported by the Defense Advanced Research Projects Agency (DARPA), John Main program manager, through Air Force Research Laboratory grant FA9453-03-C-0333 (Benjamin Henderson and Andrew Williams program monitors.) The authors wish to acknowledge William Gillespie and Scott Stacey at Delphi Chassis & Energy for supplying the MR fluid used in this investigation.

References

[1] S.C. Butler and F.A. Tito, "A broadband hybrid magnetostrictive/piezoelectric transducer aray," OCEANS 2000 MTS/IEEE, **3**:1469-1475, 2000.

[2] S. Canfield and M. Frecker, "Topology optimization of compliant mechanical amplifiers for piezoelectric actuators," *Struct. Multidisc. Optim.*, **20**:269-279, 2000.

[3] A.E. Clark, H.T. Savage and M.L. Spano, "Effect of stress on the magnetostriction and magnetization of single crystal $Tb_{0.27}Dy_{0.73}Fe_2$," *IEEE Trans. Magn.*, MAG-20(5), 1984.

[4] M.J. Dapino, R.C. Smith, L.E. Faidley and A.B. Flatau, "A coupled structural-magnetic strain and stress model for magnetostrictive transducers," *J. Intell. Mater. Sys. and Struct.*, 11(2):135–152, February 2000.

[5] M.J. Dapino, R.C. Smith and A.B. Flatau, "Structural-magnetic strain model for magnetostrictive transducers," *IEEE Trans. Magn.*, 36(3):545-556, May 2000.

[6] H. Janocha and B. Clephas, "Hybrid actuator with piezoelectric and magnetostrictive material," *Proc. Actuator '96,* pp. 304-307, Bremen, Germany, 1996.

[7] D.C. Jiles and D.L. Atherton, "Theory of the magnetisation process in ferromagnetics and its application to the magnetomechanical effect," *Journal of Physics D: Applied Physics*, 17, pp. 1265-1281, 1984.

[8] M.R. Jolly, J.W. Bender and J.D. Carlson, "Properties and applications of commercial magnetorheological fluids," *Proc. SPIE Smart Structures and Materials 1998,* San Diego, CA, March 15, 1998.

[9] L. Kiesewetter, "Terfenol-D in linear motors," *Proc. 2nd Inter. Conf. Giant Magnetostrictive Alloys,* Amter, France, 1988.

[10] C. Kormann, M. Laun and G. Klett, *Actuator 94, 4th Int. Conf. on New Actuators.* Eds. H. Borgmann and K. Lenz, Axon Technologies Consult GmbH, 1994.

[11] L.D. Mauck and C.S. Lynch, "Piezoelectric hydraulic pump development," *Journal of Intelligent Material Systems and Structures,* **11**:758-764, October 2000.

[12] J. Rabinow, "The magnetic field clutch," *AIEE Trans.*, 67, 1308-1315, 1948.

[13] M.J. Sablik and R.A. Langman, "Approach to the anhysteretic surface," *J. Appl. Phys.*, 79(8):6134-6136, 15 April 1996.

[14] J.-H. Yoo, J. Sirohi, N.A. Wereley and I. Chopra, "A magnetorheological hydraulic actuator driven by a piezopump," *Proc. of SPIE Smart Structures and Materials Symposium,* San Diego, CA, 2003.